

Supplemental Methods and Figures Legends:

METHODS

Cell line, Antibodies and Reagents. HEK 293 T cells were maintained in Dulbecco's modified Eagle's medium (DMEM) (Invitrogen Life Technologies, San Diego, CA) supplemented with 10% fetal bovine serum (FBS), 100U/ml penicillin, 200ug/ml streptomycin, and 0.25 µg/ml amphotericin B. Polyclonal antibodies against Sirt1, c-Jun or the epitope tags, HA and Myc, were obtained from Santa Cruz Biotechnology (Santa Cruz, CA). The anti-Actin, anti-Flag antibodies, as well as PMA, ionomycin and LPS, were from Sigma (Sigma, St. Louis, MO). Anti-Xpress antibody was from Invitrogen (San Diego, CA). Anti-acetyl-lysine antibody, anti-phospho-c-Jun antibodies were purchased from Cell Signaling (Danvers, MA). Anti-CD3, anti-CD28, anti-IL-2, anti-IFN-γ, anti-IL-4, anti-IL-5, PE-conjugated anti-IL-17 and FITC-conjugated anti-FoxP3 were from eBioscience (San Diego, CA). Anti-IgM F(ab')₂ was from Jackson ImmunoResearch Laboratories (West Grove, PA). JNK specific inhibitor SP600125 was obtained from CalBiochem (San Diego, CA). Antibodies against phospho-Erk1/2, phospho-JNK1/2, Erk2 and JNK1 were from Cell Signaling Technology (Billerica, MA, USA). Tamoxifen was purchased from Sigma (St. Louis, MO, USA).

Plasmids Xpress-tagged c-Jun and its mutant expression plasmids were used as reported (1). Full-length mouse Sirt1 expression plasmid was a kind gift from Eric Verdin (Gladstone Institute of Virology and Immunology, University of California, San Francisco) (2). To generate truncated mutants, fragments of the Sirt1 cDNA were amplified by PCR using linker primers that introduced *EcoRI* site at 5' end and *XbaI* site at 3' end. PCR products were digested with *EcoRI* and *XbaI*, and ligated into the pCMV-Flag expression vector (Invitrogen). All the newly generated plasmids in this study were verified by DNA sequencing. \

Mice. Sirt1 conditional knockout ($Sirt1^{loxp/loxp}$) mice (3) were purchased from Jackson Laboratories (Bar Harbor, ME). This congenic strain of mice is on C57/BL6 background and was bred with ESR-Cre transgenic mice (4). The mutant mouse estrogen receptor (ESR) does not bind natural ligand at physiological concentrations but will bind the synthetic ligand, 4-hydroxytamoxifen, which allows Cre-expression in a tamoxifen-dependent manner. A complete deletion of Sirt1 in $Sirt1^{loxp/loxp}$ ESR-Cre⁺ CD4⁺ T cells after seven days cultivation with 2 ng/ml IL-7 and 200 nM tamoxifen was confirmed by RT-PCR (data not shown).

Histological analysis of spontaneous autoimmunity and EAE. For analysis of spontaneous autoimmunity, aged (12 months or older) $Sirt1^{+/-}$ and $Sirt1^{-/-}$ mice were euthanized and their tissues including livers, lungs and kidneys were collected and frozen in OCT. 8-10 μ m sections were fixed and stained with hematoxylin-eosin (HE). For detecting autoantibody deposition in the kidney glomerules, kidney sections were stained with Alexia-488-conjugated anti-mouse IgM and IgG, respectively. Slides were then visualized with fluorescence microscopy.

For the characterization of EAE, $Sirt1^{+/-}$ and $Sirt1^{-/-}$ mice at days 17-18 (acute phase of disease) after initial immunization were euthanized and perfused with 5% formalin in 0.1M PBS. Spinal cords and cerebra were removed, immersed in the 10% formalin, and embedded in paraffin. Five- μ m sections were prepared for H&E staining. Semiquantitative histological evaluation for inflammation was performed using H&E-stained sections and scored in a blind fashion as follows: 0, no inflammation; 1, cellular infiltrate only in the perivascular areas and meninges; 2, mild cellular infiltrate in parenchymas; 3, moderate cellular infiltrate in parenchyma; and 4, severe cellular infiltrate in parenchyma. For characterization of the infiltrated lymphocytes in spinal cords, tissue sections were stained with Alexia-488-conjugated anti-CD3 and anti-CD4, respectively.

Analysis of activation-induced cell death. CD4⁺ T cells were stimulated for 24 h with anti-CD3 plus anti-CD28 to induce equal proliferation. Cells were washed and expanded for additional 3 days with IL-2. Cells were restimulated for 48 h with plate-bound anti-CD3. Cell viability was measured by staining with FITC-Annexin V and PE-conjugated 7-amino-actinomycin D (BD Pharmingen).

RT-PCR and real-time PCR. Total RNA was prepared from thymus, spleen bone marrow and lymph node using Trizol reagent (Invitrogen Corporation, Carlsbad, CA). cDNA was synthesized using oligo-dT primers and Superscript polymerase (Invitrogen) following the manufacturer's recommendations. Semi-quantitative PCR was performed to compare the expression level of Sirt1 in different tissue. The primers for Sirt1 are 5'-gttctgactggagctggggttctg-3' and 5'-tgattgtctgatggatagttac-3'. Amplification of β -actin cDNA was used as control. The primers were 5'-tgggccgctctaggcaccacaa-3' and 5'-ctctttgatgtcacgcacgatttc-3'.

Quantitative real-time RT-PCR was performed on a Prism 7000 sequence detection system (Applied Biosystems). β -actin gene was used as a reference for sample normalization. Mouse Cbl-b, Grail, EGR2, EGR3, DGK- α , IKAROS-1 primers and probe and all beta-actin primers and probe were purchased as forms of Assay-on-Demand (Applied Biosystems). Standard amplification protocol was used following the manufacture's description.

IL-2 mRNA stability assay. Mouse primary T cells were isolated and cultivated with anti-CD3 plus anti-CD28 for 24 hours. Cells were then treated with 10 μ g/ml of actinomycin D (AcD) (Sigma) for different amounts of time as indicated. Total RNA from treated cells were isolated using Trizol. The levels of mouse IL-2 mRNA were analyzed by real-time RT-PCR as described above.

Flow cytometry analysis. Single cell suspensions of thymi, spleen and lymph nodes from Sirt1^{+/-} and Sirt1^{-/-} mice pre-incubated with anti-FcγR for 10 min and were then stained with FITC-, PE- or cy-conjugated CD4, CD8, CD25, CD69, CD44 and B220 antibodies as indicated for 30 min. Cells were washed, resuspended in PBS and analyzed by FACScan and Flowjo software.

Immunofluorescence assay Primary CD4⁺ T cells were fixed with 4 % paraformaldehyde. Fixed cells were permeabilized with 0.1% Triton X-100 in PBS and incubated with anti-Sirt1 (Abcam, Cambridge, MA, USA) and anti-c-Jun antibodies followed by secondary antibody labeled with alexa-488 and Texas-Red, respectively. Nuclei were identified with 4,6-diamidino-2-phenylindole (DAPI) staining. Fluorescence was observed under fluorescence microscope.

SUPPLEMENTAL FIGURE LEGENDS:

sFig. 1. Expression of Sirt1 in immune tissues. (A) Total mRNA from mouse thymus, bone marrow, spleen and lymph nodes was isolated and used for reversely transcription into cDNA using oligo-dT primer. The cDNA levels of *Sirt1* and β -actin were analyzed by PCR. (B) The protein expression of Sirt1 in spleen (SP), thymus (TH) and lymph nodes (LN) were analyzed by western blotting using anti-Sirt1 antibody (top panel). Actin protein levels were analyzed as loading control (bottom panel).

sFig. 2. Analysis of T-cell development and activation in Sirt1^{-/-} mice. Cells from thymus, spleen and lymph nodes were isolated from Sirt1^{+/-} and Sirt1^{-/-} mice. (A) The cell surface expression of CD4 and CD8, or CD3 and B220, was analyzed. (B) Expression of CD69, CD44 and CD25 were analyzed by flow cytometry, gating on CD4⁺ T cells in lymph nodes. (C) The expression of CD3 ϵ and TCR β chains in the spleen and lymph nodes were analyzed by flow cytometry. Data indicate the percentage/mean fluorescence.

sFig. 3. Sirt1 inhibits T cell activation. (A) CD4⁺ T cells were purified from Sirt1^{loxp/loxp}ESR-Cre (KO) and Sirt1^{+/+}ESR-Cre (WT) mice. Cells were cultured with IL-7 (2ng/ml) and tamoxifen (200nM) for seven days and then washed. Cells were stimulated with anti-CD3 or with anti-CD3 plus anti-CD28 and their proliferation was analyzed. Representative results from two independent experiments were shown. (B) CD4⁺ T cells were purified from Sirt1^{+/-} and Sirt1^{-/-} mice and infected with retrovirus that contains empty vectors (MIG) or Sirt1 gene (MIG-Sirt1). GFP⁺ positive cells were rested and restimulated with anti-CD3 or anti-CD3 + anti-CD28. Cell proliferation was analyzed and results are representative for three independent experiments.

sFig. 4. Sirt1-deficient APC does not contribute to the hyper-proliferation of Sirt1^{-/-} CD4 T cells.

(A) CD4⁺ T cells and APCs were prepared from Sirt1^{-/-} and Sirt1^{+/-} spleen, respectively. Cells were cocultured in the presence of anti-CD3 antibody as indicated. CD4⁺ T cell proliferation was analyzed. (B) CD11c⁺ cells in spleen or lymph nodes were gated, their expressions of CD80 and CD86 were analyzed. Data indicate the percentage/mean fluorescence.

sFig. 5. IL-2 productions by Sirt1^{+/-} and Sirt1^{-/-} after anergic induction. (A & B) *In vivo* tolerance was induced by treatment of Sirt1^{+/-} OT-II and Sirt1^{-/-} OT-II mice with OVA323-339 peptides, or with PBS as a control, by tail vein injection. Total lymphocytes from lymph nodes were isolated from treated mice and IL-2 production was analyzed. (C) Sirt1^{-/-} and Sirt1^{+/-} CD4⁺ T cells were undergone *in vitro* anergy induction and then re-stimulated with anti-CD3 plus anti-CD28. Their IL-2 production was determined.

sFig. 6. T cell anergy study using purified CD4⁺ T cells. Sirt1^{+/-} OT-II and Sirt1^{-/-} OT-II mice were treated with OVA323-339 or PBS as a control. CD4⁺ T cells were isolated from the treated mice and co-cultured with Sirt1^{+/-} APCs in the presence of different amounts of OVA peptide. The proliferation of CD4⁺ T cells was analyzed. Error bars represent data from three mice.

sFig. 7. Sirt1 restores anergy induction of Sirt1^{-/-} CD4⁺ T cells. (A) CD4⁺ T cells from Sirt1^{-/-} mice were purified and infected with retrovirus that carries either control vector (MIG) or Sirt1 genes (MIG-Sirt1). Infected cells were rested and treated with 1 ug/ml ionomycin (IONO) for 16 hours and then washed. Cells were restimulated with anti-CD3 plus anti-CD28 and their proliferation were analyzed. Representative result from two independent experiments was shown. (B) CD4⁺ T cells were purified from Sirt1^{loxp/loxp} ESR-Cre (KO:ESR-Cre+Tam) and Sirt1^{+/+} ESR-Cre (WT:ESR-Cre+Tam) mice. Cells were cultured with anti-CD3 plus anti-CD28, IL-2 (5ng/ml) and tamoxifen (200nM) for seven days and then

washed. Expanded cells were treated with 1 µg/ml ionomycin (IONO) or without (rested) for 16 hours and then washed. Cells were restimulated with anti-CD3 plus anti-CD28 and their proliferation was analyzed by ³H-thymidine incorporation.

sFig. 8. Activation-induced cell death of Sirt1^{-/-} T cells. Primary CD4⁺ T cells were purified and expanded with anti-CD3 plus anti-CD28 in the presence of IL-2 for five days. Expanded cells were restimulated with anti-CD3, anti-CD3 plus anti-CD28 or PMA plus ionomycin for additional 16 hours. The apoptosis cells were analyzed by annexin V and 7-AAD staining.

sFig. 9. Sirt1 does not affect the T cells homeostasis. CD4⁺ T cells were stained with CFSE and adoptively transferred into T cell deficiency mice with 5X10⁶ cells per mouse. One week after the adoptive transfer, mice were euthanized. Splenocytes were isolated and the CD4⁺ CFSE-labeled cells were analyzed by flow cytometry. Four pairs of mice were analyzed and representative data were shown.

sFig. 10. Gene expression analysis in Sirt1^{+/-} and Sirt1^{-/-} T cells under anergic stimulation. CD4⁺ T cells from Sirt1^{-/-} and Sirt1^{+/-} mice were expanded, rested and treated with 1 µg/ml ionomycin for 16 hours. Total RNAs were isolated from the rested and ionomycin-treated cells. The expression levels of Cbl-b, DGKa-1, EGR2, EGR3, Grail and IKAROS-1 were analyzed by real-time PCR using β-actin as a control. Results are representative for two independent experiments.

sFig. 11. MAPK activation in Sirt1^{-/-} T cells. Primary CD4⁺ T cells were purified from Sirt1^{-/-} and Sirt1^{+/-} mice and stimulated with anti-CD3 or anti-CD3 plus anti-CD28 for 5 min. The activation of Erk (top panel) and JNK (third panel) was analyzed using specific antibodies against their phosphorylated forms. The same membrane was reprobbed with anti-Erk2 and anti-JNK1, respectively.

sFig. 12. The effects of c-Jun phosphorylation on its interaction with Sirt1. (A) HEK 293 cells were transfected with c-Jun and Sirt1. Transfected cells were treated with JNK-specific inhibitor SP600125 (SP) for 16 hour. Sirt1 protein in the treated cells was immunoprecipitated with anti-Sirt1 antibodies. The interaction of c-Jun with Sirt1 in these immunoprecipitates was detected with anti-c-Jun antibody (top panel). The same membrane was reprobed with anti-Sirt1 antibody (2nd panel). The levels of phosphorylated c-Jun, total c-Jun and Actin control in the whole cell lysates were detected with each specific antibody (bottom 3 panels). (B & C) Sirt1 was co-transfected with or without Xpress-tagged c-Jun or each of c-Jun mutants. c-Jun protein was immunoprecipitated with anti-Xpress antibody, the interaction of Sirt1 with c-Jun or its mutants was detected with anti-Sirt1 (top panel), and the same membrane was reprobed with anti-Jun antibody (middle panel). The expression of Sirt1 in the whole cell lysates was confirmed by western blotting (bottom panel).

sFig. 13. The effects of T-cell activation signaling on Sirt1 and c-Jun colocalization. Mouse primary T cells were unstimulated (top panel) or stimulated (bottom panel) with anti-CD3 plus anti-CD28 for 24 hours. Cells were cyo-spun onto slide and fixed. The expression of c-Jun (red) and Sirt1 (green) was immunostained with anti-c-Jun and anti-Sirt1, respectively. The nuclear DNA was stained with DAPI. The selected cells represent more than 85% of the population.

sFig. 14. Co-localization of Sirt1 with c-Jun in anergic T cells. Mouse primary T cells were expanded, and then rested (top panel) or treated with ionomycin for 16 hours for anergy induction (bottom panel). Colocalization of Sirt1 with c-Jun was analyzed as described in sFig. 15.

sFig. 15. Analysis of the spontaneous autoimmune response in Sirt1^{-/-} mice. (A) The concentration of ANA in sera from Sirt1^{-/-} and Sirt1^{+/-} mice was examined by ELISA. Data were analyzed by the Student's *t* test. (B) Fixed NIH3T3 mouse fibroblasts cells were stained with a 1:500 dilution of sera from Sirt1^{-/-} and Sirt1^{+/-} mice, followed by Alexa-488 conjugated anti-mouse IgG antibody. Immunostained cells were visualized by fluorescence microscopy. (C) Kidney sections of Sirt1^{-/-} and Sirt1^{+/-} mice were stained with Alexa-488-conjugated anti-mouse IgM (top panels) and anti-mouse IgG (bottom panels). (D) Tissue sections of liver, kidney and lung from Sirt1^{-/-} and Sirt1^{+/-} mice were stained with H & E and images were taken. X200.

sFig. 16. Analysis of the spontaneous autoimmune response in Sirt1^{-/-} mice. (A) The concentration of ANA in sera from Sirt1^{-/-} and Sirt1^{+/-} mice was examined by ELISA. Data were analyzed by the Student's *t* test. (B) Fixed NIH3T3 mouse fibroblasts cells were stained with a 1:500 dilution of sera from Sirt1^{-/-} and Sirt1^{+/-} mice, followed by Alexa-488 conjugated anti-mouse IgG antibody. Immunostained cells were visualized by fluorescence microscopy. (C) Kidney sections of Sirt1^{-/-} and Sirt1^{+/-} mice were stained with Alexa-488-conjugated anti-mouse IgM (top panels) and anti-mouse IgG (bottom panels). (D) Tissue sections of liver, kidney and lung from Sirt1^{-/-} and Sirt1^{+/-} mice were stained with H & E and images were taken. X200.

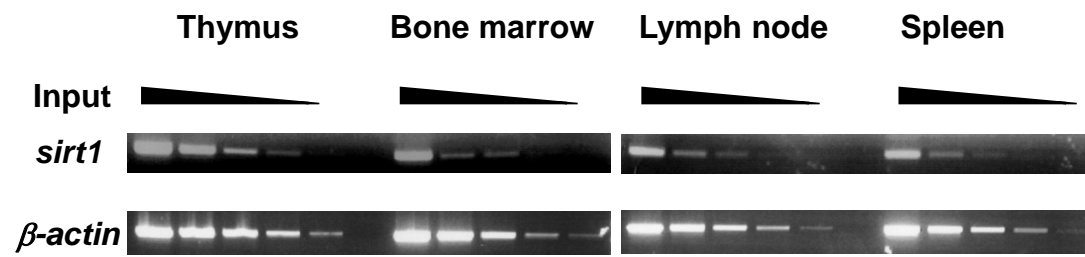
References:

1. Lee, S., B. Gao, and D. Fang. 2008. FoxP3 maintains Treg unresponsiveness by selectively inhibiting the promoter DNA-binding activity of AP-1. *Blood* 57:988-1007.
2. Pagans, S., A. Pedal, B.J. North, K. Kaehlcke, B.L. Marshall, A. Dorr, C. Hetzer-Egger, P. Henklein, R. Frye, M.W. McBurney, H. Hruby, M. Jung, E. Verdin, and M. Ott. 2005. SIRT1 regulates HIV transcription via Tat deacetylation. *PLoS Biol* 3:e41.

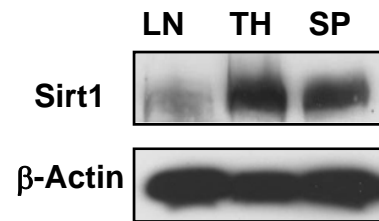
3. Li, H., G.K. Rajendran, N. Liu, C. Ware, B.P. Rubin, and Y. Gu. 2007. SirT1 modulates the estrogen-insulin-like growth factor-1 signaling for postnatal development of mammary gland in mice. *Breast Cancer Res* 9:R1.
4. Metzger, D., J. Clifford, H. Chiba, and P. Chambon. 1995. Conditional site-specific recombination in mammalian cells using a ligand-dependent chimeric Cre recombinase. *Proc Natl Acad Sci U S A* 92:6991-6995.

Supplemental Fig. 1

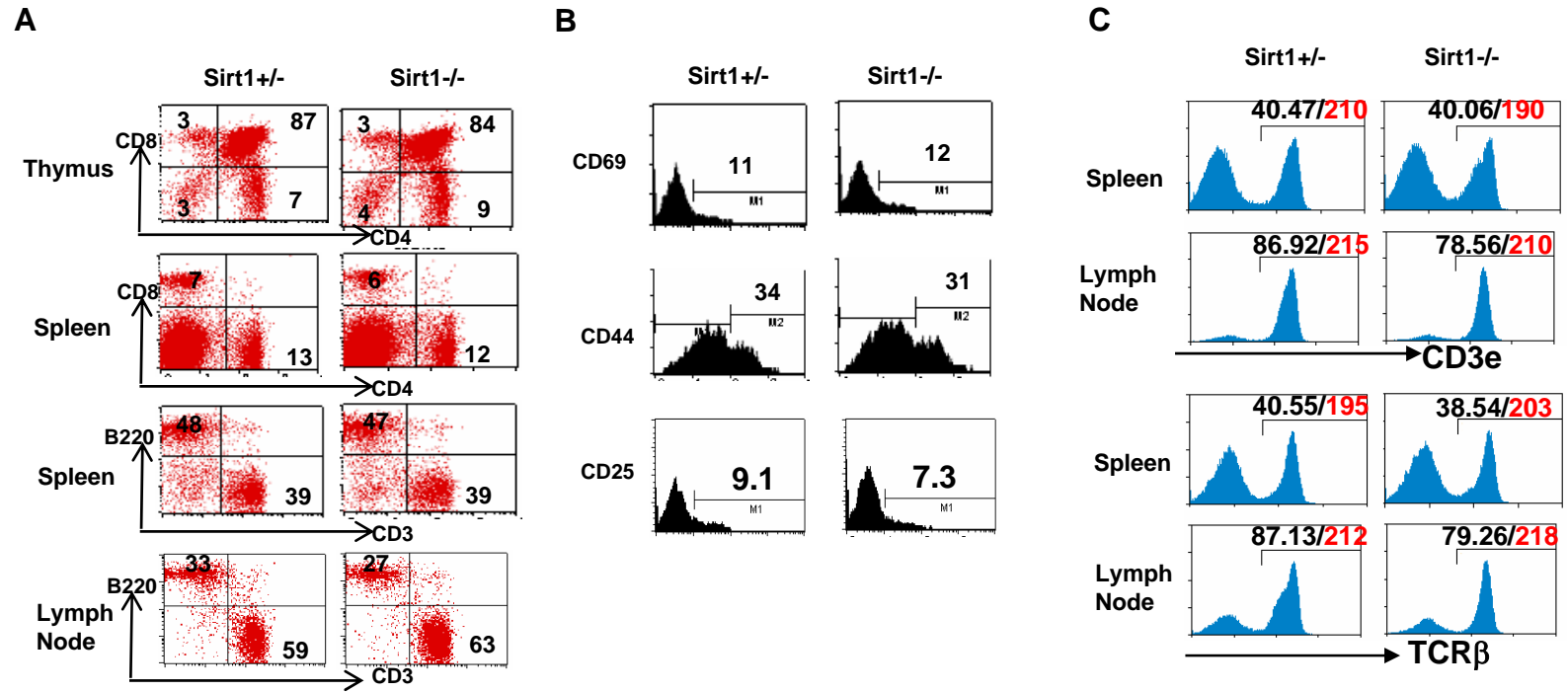
A



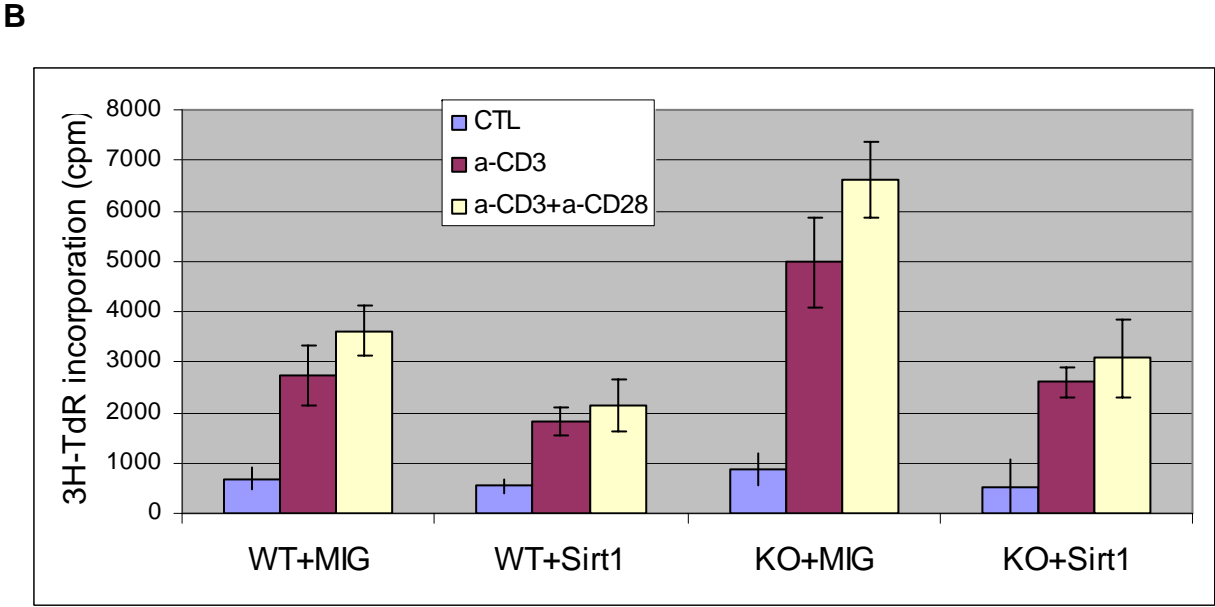
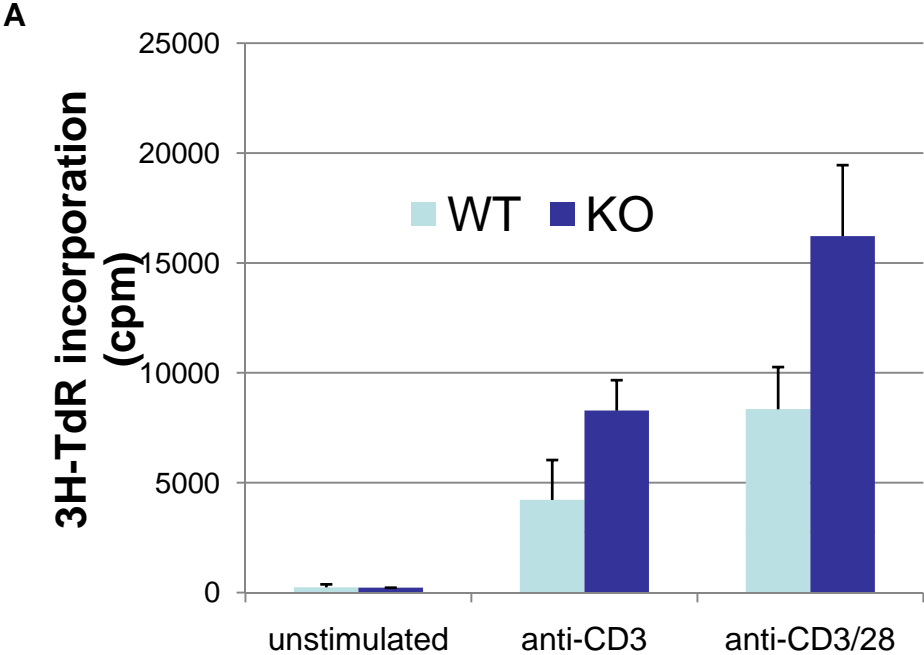
B



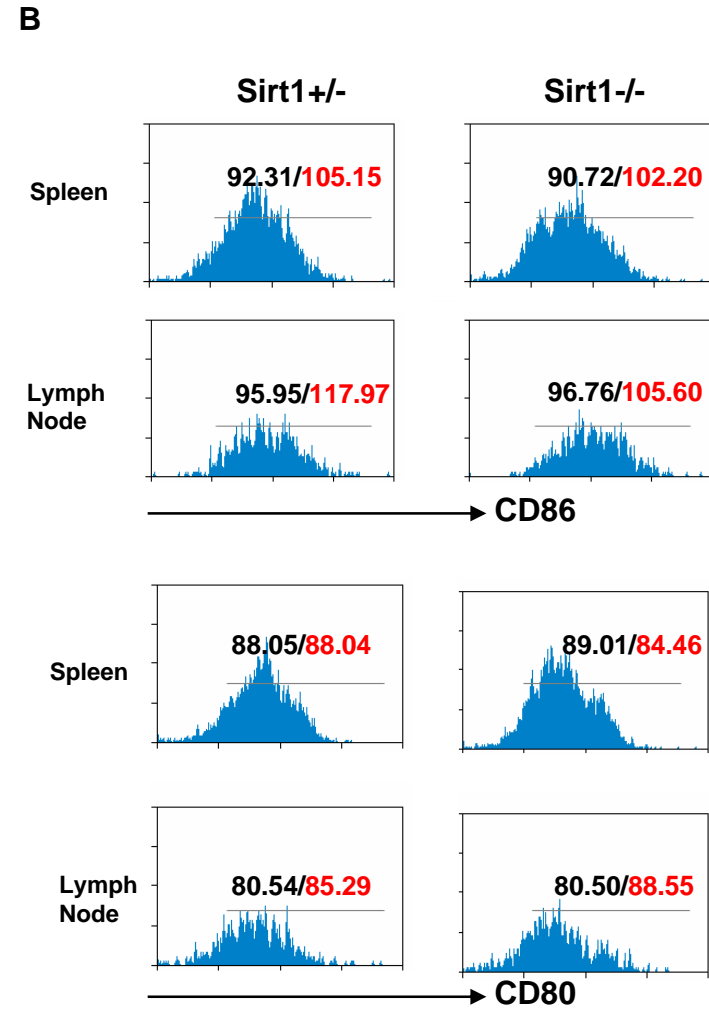
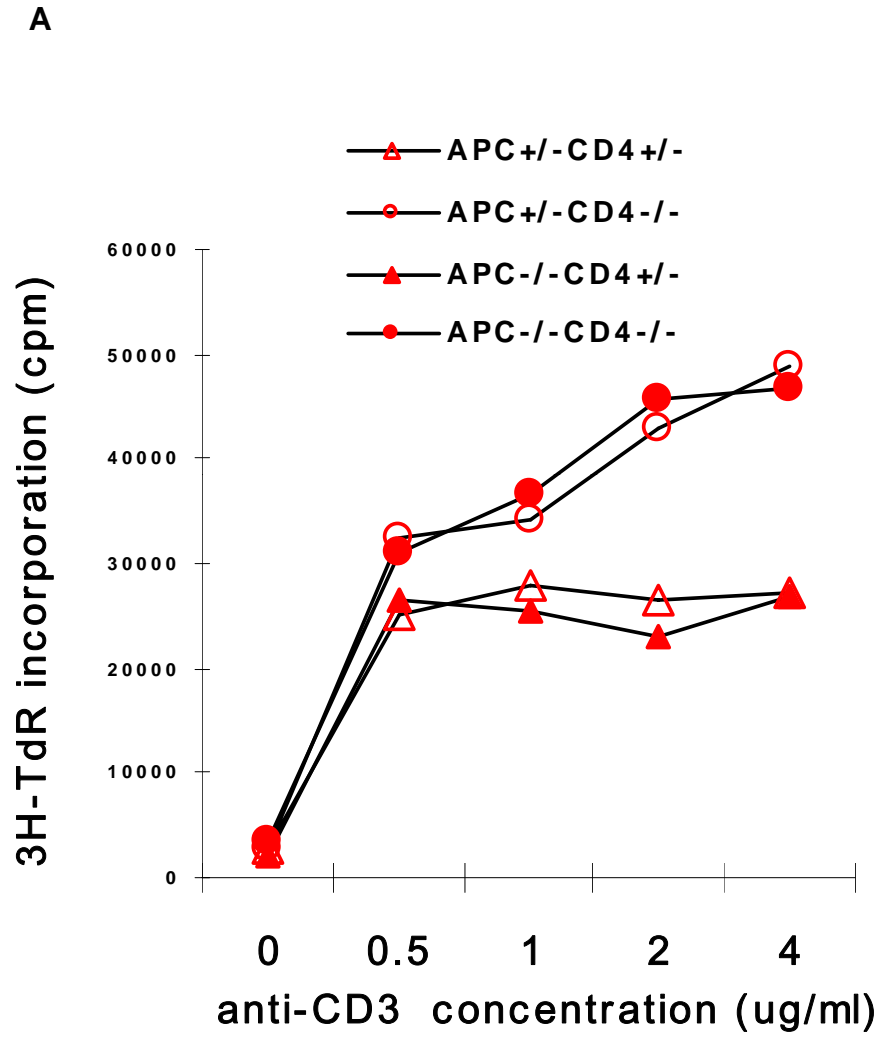
Supplemental Fig. 2



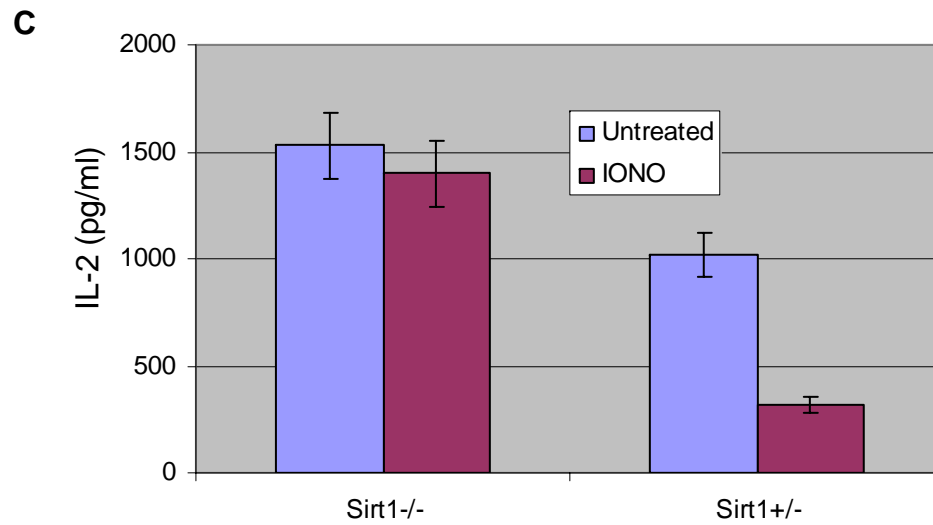
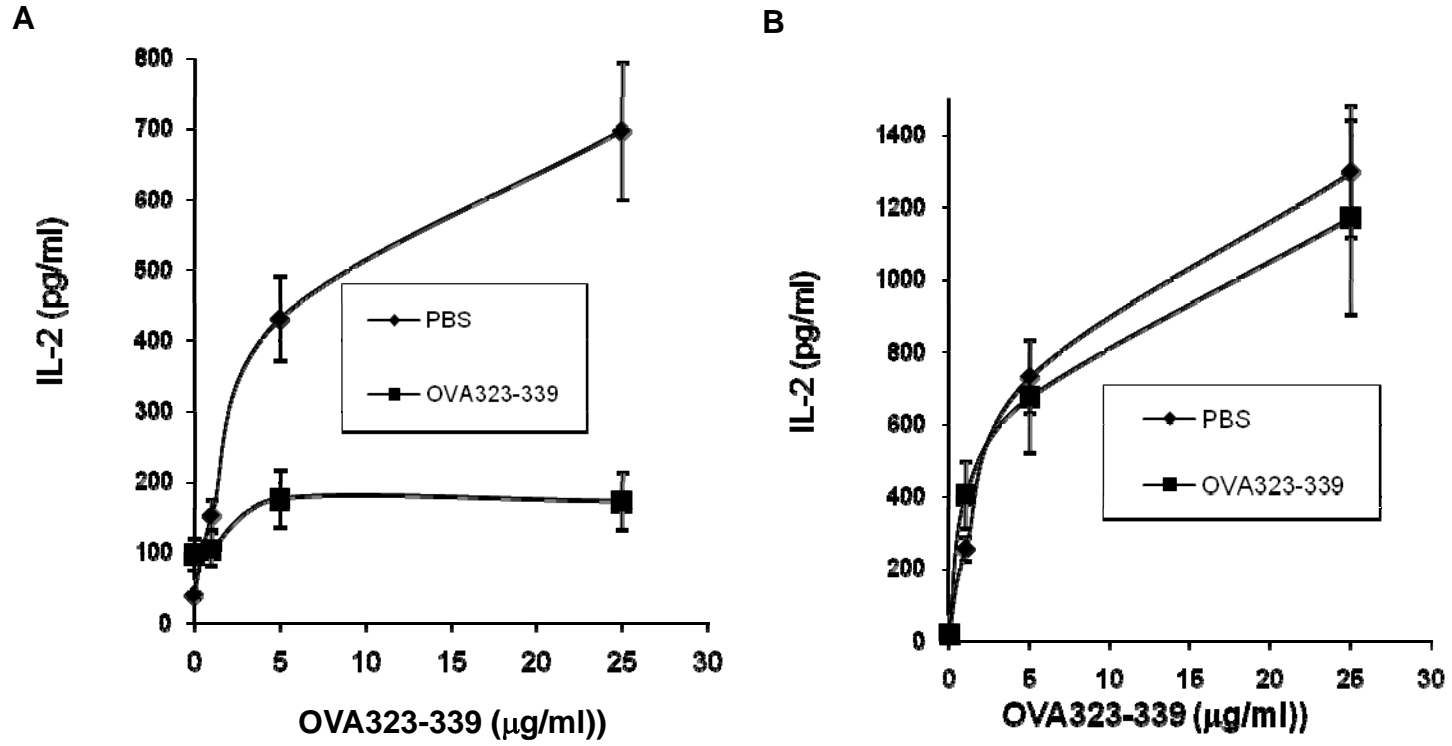
Supplemental Fig. 3



Supplemental Fig. 4

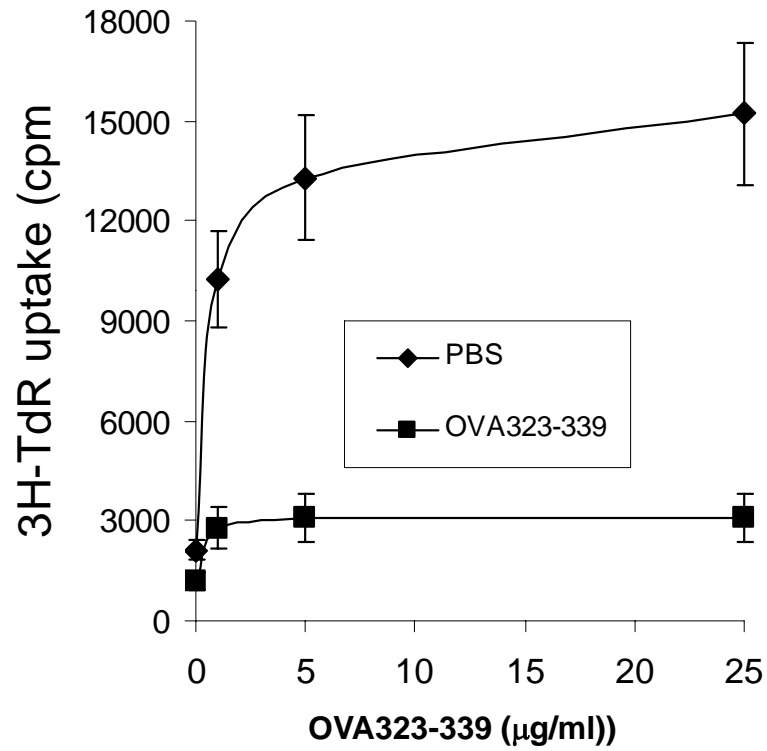


Supplemental Fig. 5

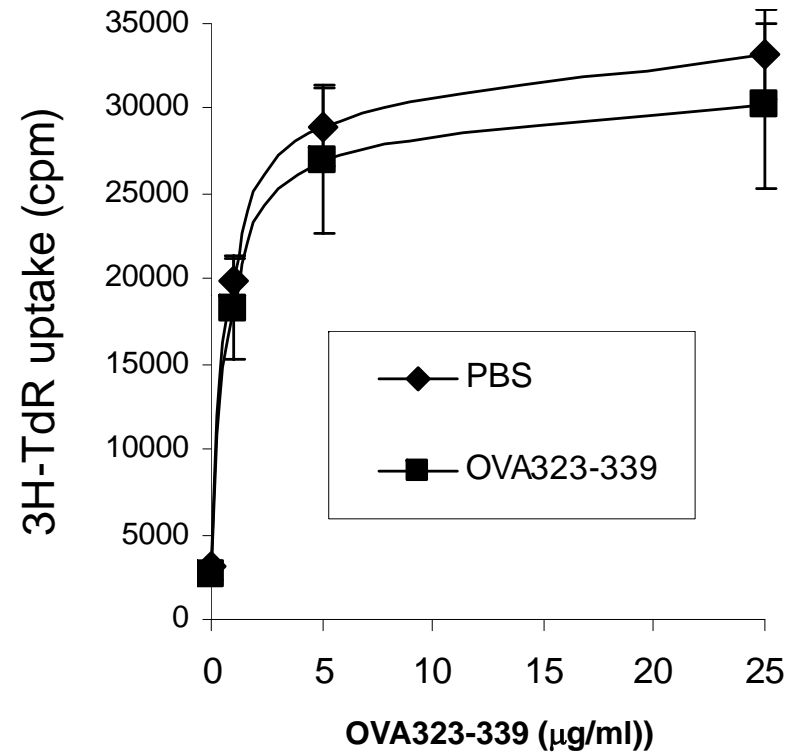


Supplemental Fig. 6.

A

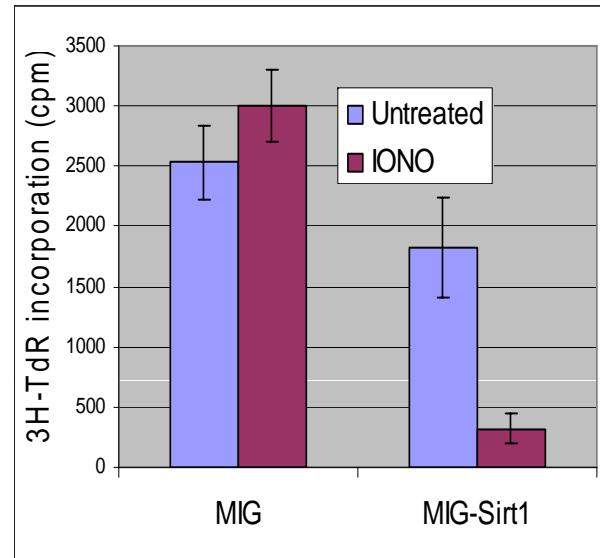


B

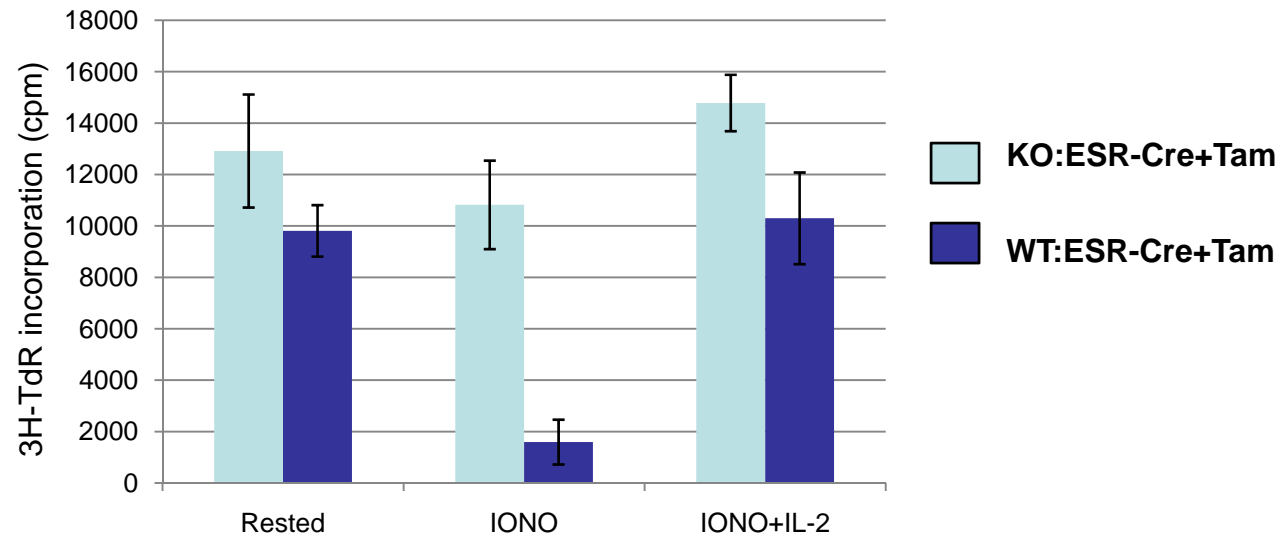


Supplemental Fig. 7

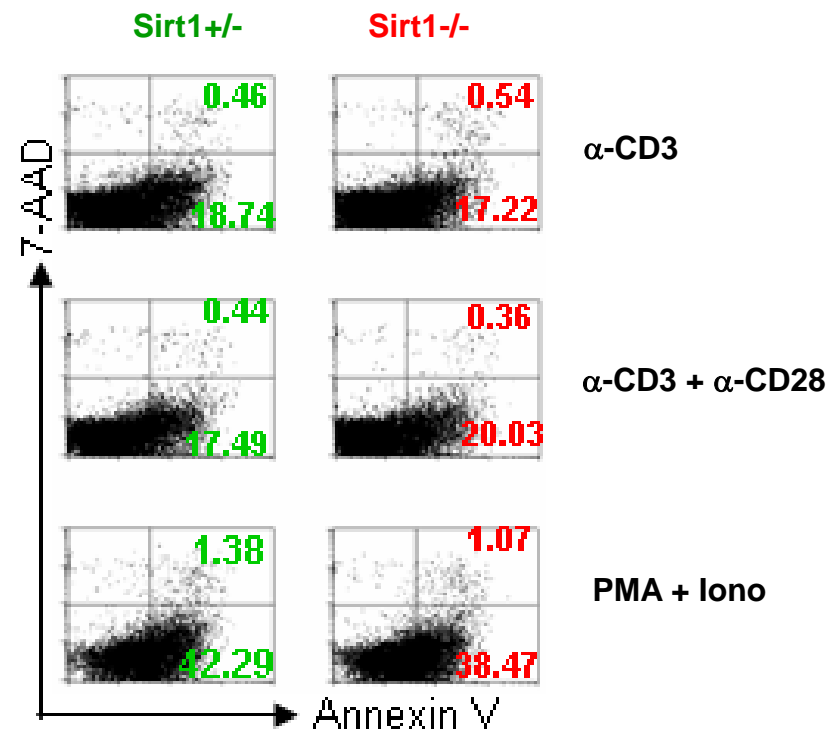
A



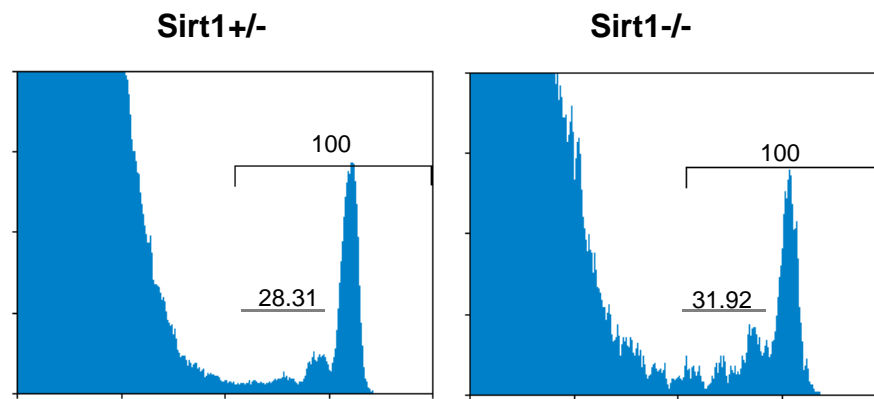
B



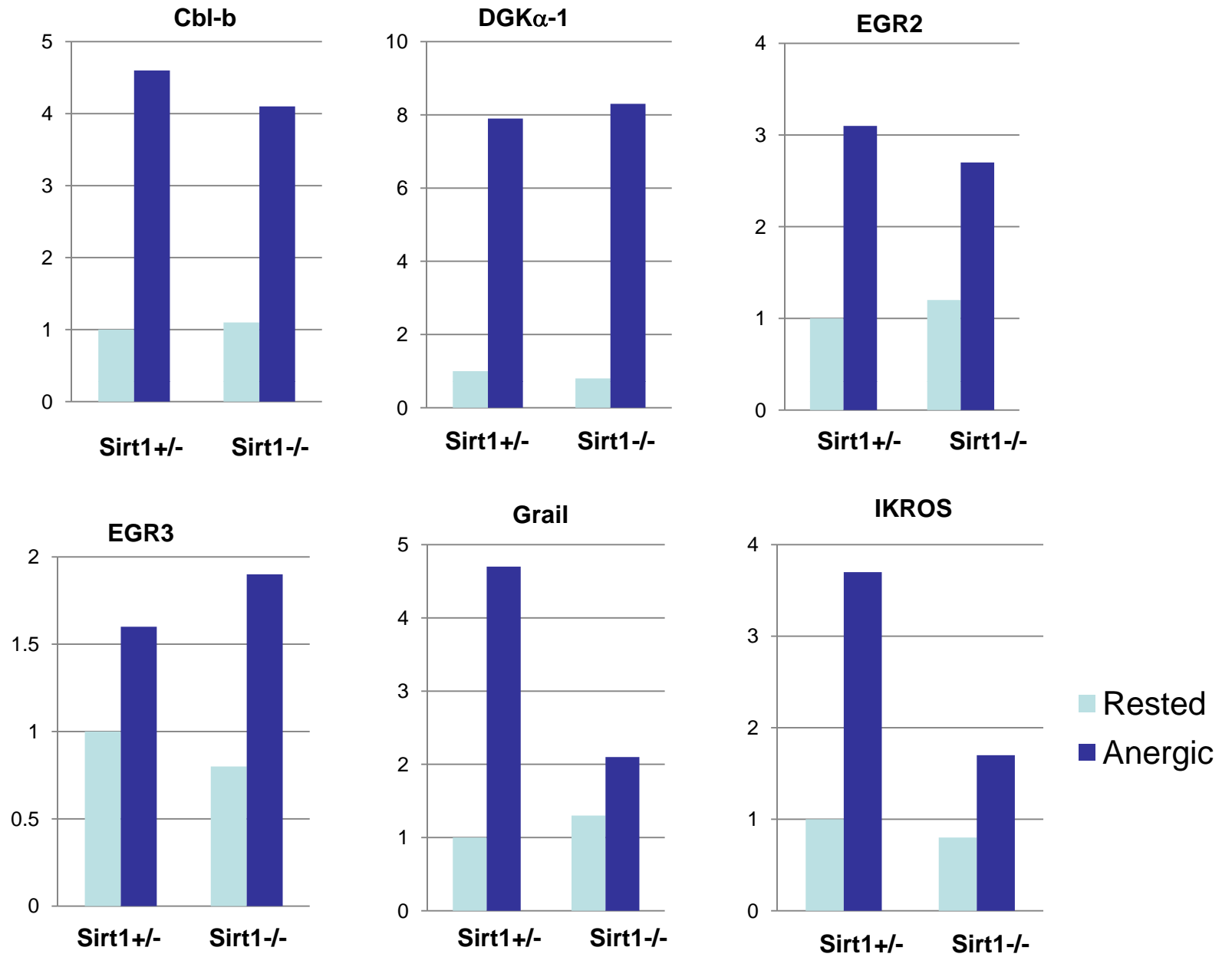
Supplemental Fig. 8



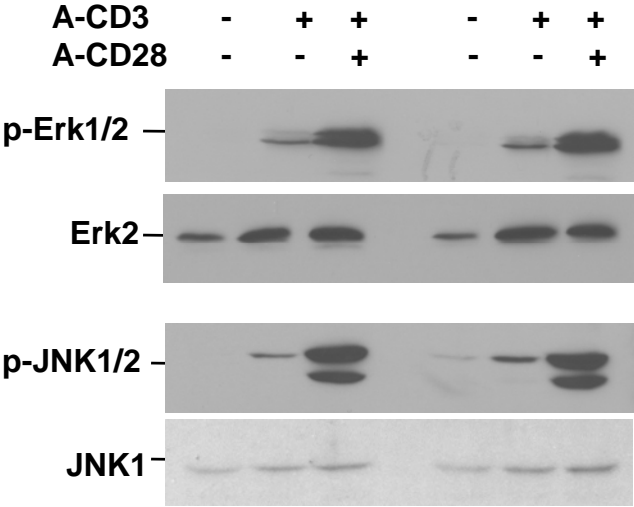
Supplemental Fig. 9



Supplemental Fig. 10

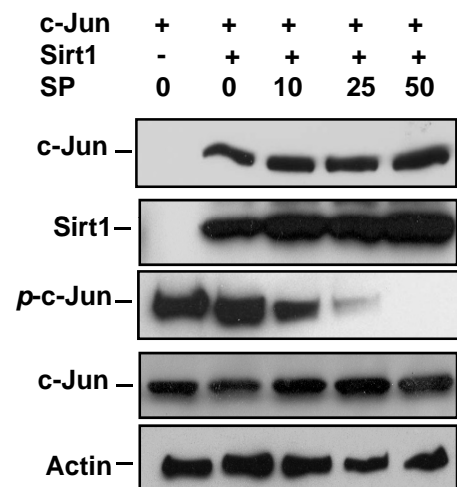


Supplemental Fig. 11

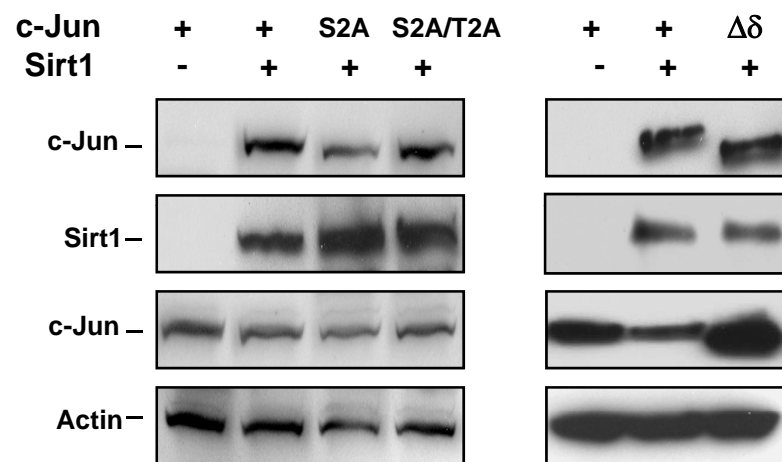


Supplemental Fig. 12

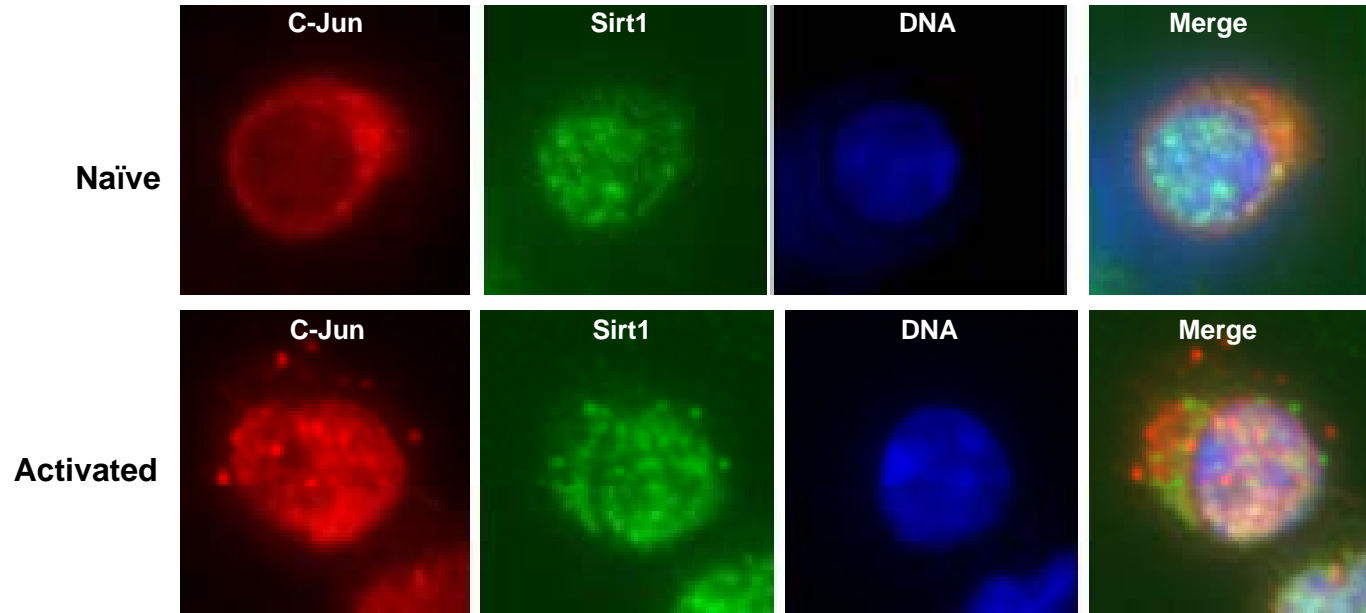
A



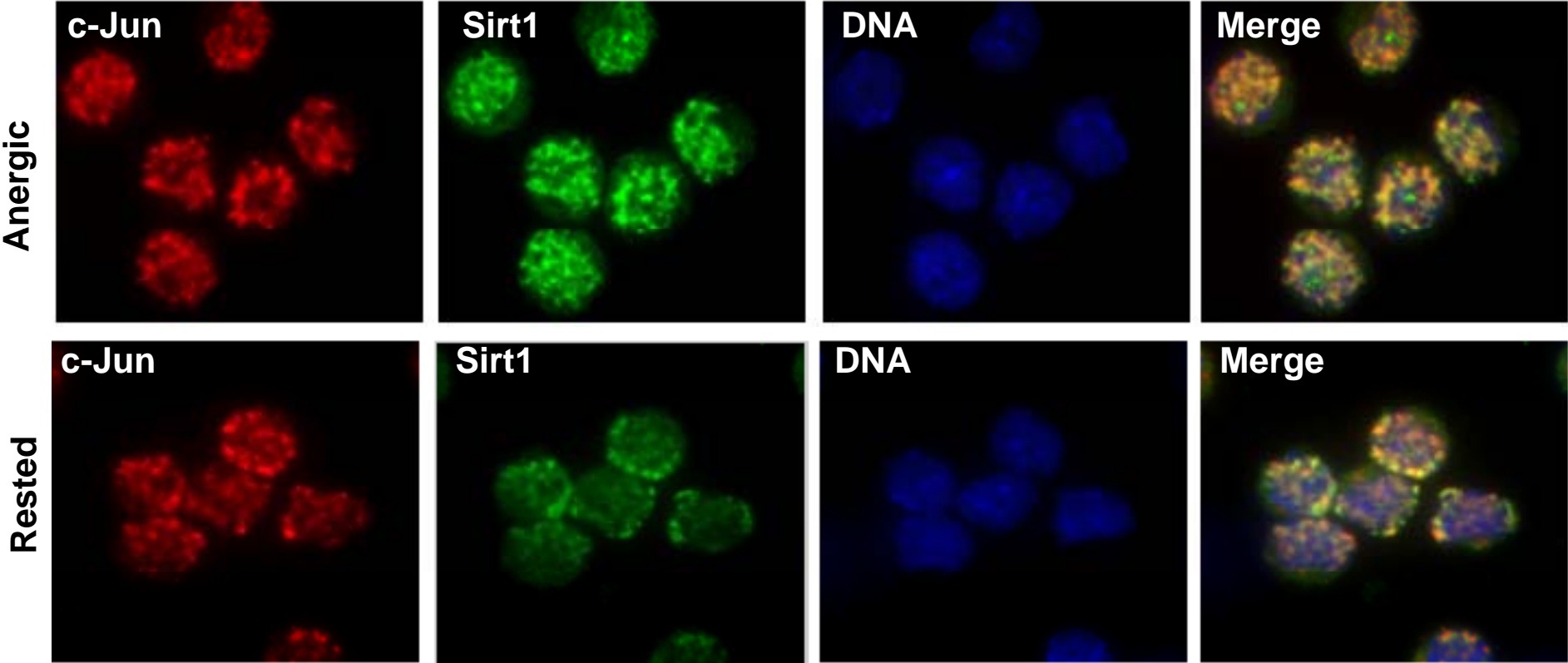
B



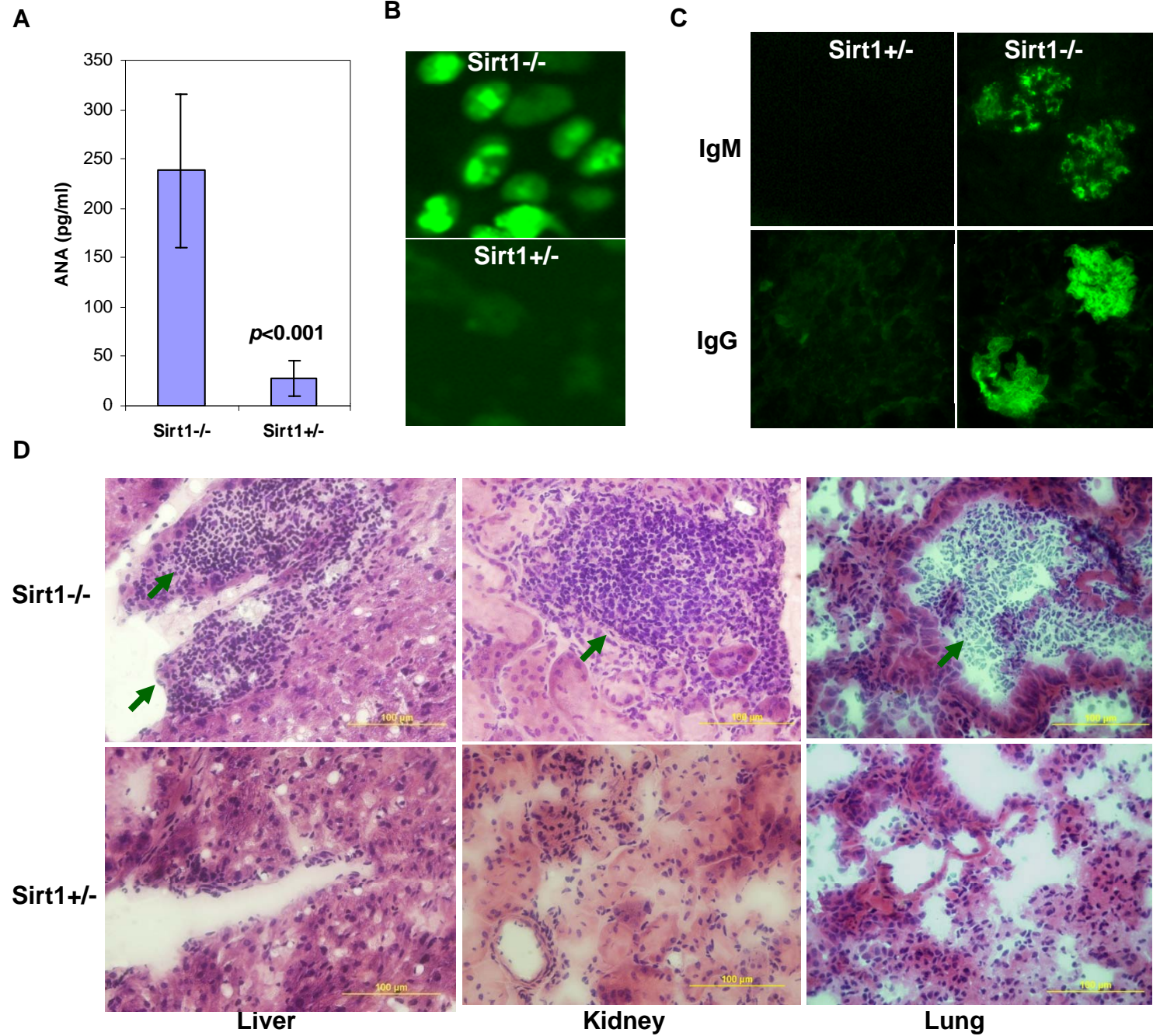
Supplemental Fig. 13



Supplemental Fig. 14

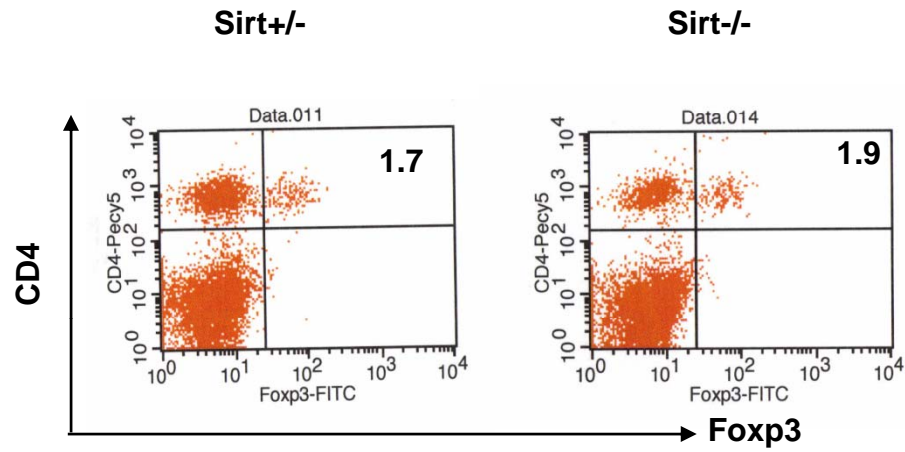


Supplemental Fig. 15

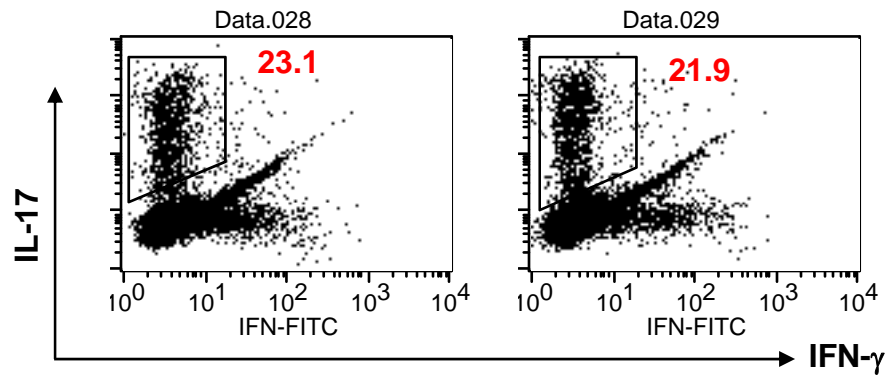


Supplemental Fig. 16

a



b



c

